Journal of the Ceramic Society of Japan 128 [12] 1018-1023 2020
DOI http://doi.org/10.2109/jcersj2.20181

JCS-Japan

FULL PAPER

# Flash sintering for $BaTiO_3$ with square alternating current field including zero-field duration

**Ryosuke UMEMURA[1], Tomoharu TOKUNAGA[1] and Takahisa YAMAMOTO[1,†]**

[1]Nagoya University, Department of Materials Design Innovation Engineering, Furocho, Chikusa-ku, Nagoya 464–8603, Japan

**The shrinkage behavior of barium titanate ($BaTiO_3$) green compacts during flash sintering with a square alternating current (AC) field including a zero-field duration (AC-pulse wave) was investigated. It was found that an AC-pulse wave is effective for the densification of $BaTiO_3$ green compacts without reduction and discharge, which is confirmed by transmission electron microscopy and electron energy loss spectroscopy. $BaTiO_3$ sintered polycrystal was obtained at a furnace temperature of 1000 °C by the optimal AC-pulse conditions of 285 V/cm at 250 Hz and a duty ratio of 30 %. A waveform with alternating polarity and the inclusion of a zero-field duration is shown to be possibly useful for flash sintering of oxide materials including altervalent cations.**


Key-words : $BaTiO_3$, $SrTiO_3$, Flash sintering, Discharge, Microstructure

[Received September 9, 2020; Accepted October 12, 2020]

## 1. Introduction

The flash sintering technique, which was developed by Raj's research group, is very effective to greatly enhance the shrinkage rates.[1)] This sintering technique uses an electric field to enhance the shrinkage rate of green compacts, which can be categorized as a field assisted sintering technique (FAST). The characteristic point of flash sintering is the occurrence of a specimen electric current spike during the heating of green compacts, which is called a flash event. A huge shrinkage occurs steeply with this flash event, and the sintering process is completed immediately.[1)] So far, the effectiveness of the flash sintering technique has been confirmed for various kinds of ceramics but not pure alumina.[2)–5)] However, the high densification of compacts is not always achieved by this sintering technique. For example, the occurrence of discharge is a fatal barrier for the completion of shrinkage in $BaTiO_3$.[6),7)] M'Peko et al. reported the criterion of applied electric fields for discharge.[6)] According to their report, the critical electric current ranges from approximately 20 mA/mm$^2$ at 100 V/cm to approximately 9 mA/mm$^2$ at 700 V/cm, which depends on the magnitude of the direct current (DC) fields. The current flow in a green compact localizes to form discharge damage in the flash conditions above this range. As a result, the final linear shrinkages are limited below the critical limiting current. A relative density of 97.1 % was obtained at a flash condition of 150 V/cm by controlling the balance between the electric field and limiting current, with conditions of 60 mA, 15 min and 900 °C, using green compacts with a dog-bone shape.[6)] When discharge occurred, a non-uniform microstructure, which included abnormal grains, secondary phases and so on, was formed in/near the portion damaged owing to the discharge.[6)–8)] The grain size became larger near the discharged holes. Further, Ba-less compounds were often formed as the secondary phases, which resulted from the vaporization of some of the Ba from $BaTiO_3$ owing to the higher Joule heat arising from the current concentration.

The occurrence of the discharge is discussed in terms of the reduction phenomena which occurs during flash sintering with DC fields. DC fields enforce a one-directional flow of oxygen ions. The generation of the one-directional flow of oxygen ions forms excess oxygen vacancies, which increases the electrical conductivity of n-type conduction.[9)] As a result, a biased electric current flow occurs which finally leads to discharge. The formation of oxygen vacancies decreases the valence of Ti cations. Nakagawa et al. confirmed the reduction of Ti cations using electron energy loss spectroscopy (EELS) performed for grain boundaries of $BaTiO_3$ polycrystals consolidated under DC electric fields.[10)] Although their electric field and current condition were mild compared with those used in flash sintering, they reported that a fine structure change of Ti $L_{23}$-edges showing reduction occurred. To decrease the effect of reduction, a waveform with alternating polarity can be considered to be preferable. Thus, we paid attention to a modified alternative square waveform including a zero-field duration, which is expected to recover excess oxygen vacancies during the zero-field duration.

In order to obtain $BaTiO_3$ polycrystals with tetragonal phase by flash sintering, it must be necessary to avoid the transformation from cubic to hexagonal phase, which

† Corresponding author: T. Yamamoto; E-mail: yamamoto.takahisa@material.nagoya-u.ac.jp

exists around 1460 °C.[11] This transformation temperature is decreased to around 1300 °C by reducing atmosphere.[12] Thus, to obtain densified and uniform structured $BaTiO_3$ polycrystals using the flash sintering technique, it is necessary to use a suitable waveform to suppress discharging and to apply an electric field under which the Joule heating will not form the hexagonal phase. Further, we aimed to obtain densified $BaTiO_3$ polycrystals at around 1000 °C from a viewpoint of an electric furnace using nichrome heaters.

In this study, we investigate the shrinkage behavior of $BaTiO_3$ green compacts flash sintered with a controlled waveform and perform microstructure analysis by transmission electron microscopy (TEM) and EELS.

## 2. Experimental procedure

Commercially available high purity $BaTiO_3$ powder (BT-01, Ba/Ti = 1.000, SAKAI CHEMICAL INDUSTRY CO., LTD.) was used as a raw powder. In this study, we used a green compact with a rectangular shape, which was thermally restricted because of a direct contact between the electrode and green compact. Green compacts with a cross section of 5 × 5 $mm^2$ and length of 15 mm were prepared by uniaxial pressing at 75 MPa followed by cold-isostatic pressing at 100 MPa. Linear shrinkages with electric fields were measured by a high-temperature dilatometer (EVO2 TMA8301, Rigaku, Japan) which was modified to apply electric fields to the green compacts.[13] Electric fields were applied to the green compact in the longitudinal direction after thin Pt sheets were fixed as electrodes on both 5 × 5 $mm^2$ faces of the green compacts with Pt paste. In this study, electric fields with alternating polarity were used as the applied fields on the green compacts, as shown in **Fig. 1**. The waveform included two kinds of durations; one is a rectangular shape, as indicated by A, and the other is a zero field, as indicated by B. The polarity of the rectangular wave changed between positive and negative alternatively. Inclusion of the zero-field duration was expected to recover excess oxygen vacancies, i.e., to decrease the reduction during the application of the electric field. Hereafter, this modified waveform will be termed as the AC pulse. The duty ratio of the AC pulse was defined by the ratio of $2A/\lambda$, as indicated in Fig. 1. For example, the frequency was 25 Hz when the duration time at A and B were set to be 0.01 s.

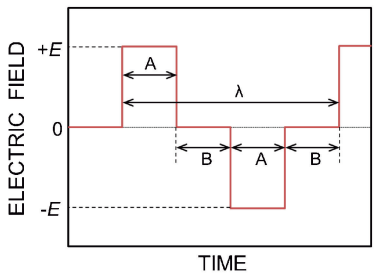


Fig. 1. A schematic illustration showing the waveform used in the present study. Duration at A is a square pulse (DC component), B is the zero field and $\lambda$ is one wavelength.

It is necessary to determine the magnitude of the electric fields of the AC pulse wave, as indicated by $E$ in Fig. 1, which induces a flash event at 1000 °C because this study aims to obtain the densification of $BaTiO_3$ compact around 1000 °C. According to previous study,[6] a flash event occurs around 1000 °C at DC field of about 140 V/cm. In the case of the present wave, the wavelength includes the zero-field duration of B so that the magnitude of the field must be calculated as the root mean square value to adjust the DC field of 140 V/cm. As indicated in Fig. 1, the electric power of the AC pulse with a field magnitude of $E_{\mathrm{AC\ pulse}}$ and frequency of $f$ which are included in one wavelength is as follows,

$$\frac{1}{f} \times d \times \frac{{E_{\mathrm{AC\ pulse}}}^2}{R} \tag{1}$$

where $d$ is the duty ratio as expressed by $2A/\lambda$, as indicated in Fig. 1, and $R$ is the resistance of a green compact below the occurrence of a flash event. The electric power of the DC field, $E_{\mathrm{DC}}$, included in a duration time of $1/f$ is as follows,

$$\frac{1}{f} \times \frac{{E_{\mathrm{DC}}}^2}{R} \tag{2}$$

Then, the magnitude of the electric field $E_{\mathrm{square}}$ of the AC pulse corresponding to $E_{\mathrm{DC}}$ can be obtained as follows,

$$E_{\mathrm{square}} = \frac{E_{\mathrm{DC}}}{\sqrt{d}} \tag{3}$$

Here, $E_{\mathrm{DC}} = 140$ V/cm, then, $E_{\mathrm{AC\ pulse}} = 200$ V/cm in the present AC pulse at a duty ratio of 50 %.

The duty ratio and frequency of the AC pulse were changed from 10 to 70 % and from 0.25 to 2500 Hz, respectively. For comparison, a square wave without a zero-field duration and a DC field were also used. The waveforms of the AC pulse and square waves were generated by a function generator (eK-FGJ; Matsusada Precision, Inc., Japan) linked to a high voltage AC power supply (POPF-300-4; Matsusada Precision, Inc., Japan). For the DC field, a high voltage DC power supply (HEP-3-2100; Matsusada Precision, Inc., Japan) was used. The detailed electric field conditions will be described in the respective figures.

The green compacts were heated from room temperature to the flash temperature, at which the specimen electric current exhibited a spike, i.e., a flash event, at a constant heating rate of 300 °C/h in air. The limiting value of specimen electric current was pre-set in the power supplies as described above. When the specimen electric current reached the pre-set limiting current value, the heating process was quitted and the furnace temperature was kept at the flash temperature by switching a furnace temperature controller manually. After that, the furnace temperature was maintained for 1 h by controlling the specimen electric current at a limiting value and then cooled without any electric field.

Microstructures of the flash sintered compacts were analyzed by using a high resolution scanning transmission

electron microscope (STEM, ARM-200FC, JEOL Ltd.) operated at 200 kV. Thin foils for STEM observation were prepared by a conventional technique including mechanical grinding, polishing, and Ar ion-milling. EEL analysis was performed using an imaging filter (GIF Quantum ER, GATAN Inc.), which operated at an energy dispersion of 0.1 eV/ch, attached to STEM. EEL spectra were obtained in a probe mode with a probe size of approximately 10 nm to decrease the irradiation damage caused by the incident electron beam.

The crystal structures after flash sintering were measured by X-ray diffraction (XRD; D2 PHASER; Bruker Corp.) with the Cu K$\alpha$ line.

## 3. Results and discussion

**Figure 2**(a) shows the shrinkage behavior of green compacts under an AC-pulse field as a function of furnace temperature. The AC pulse field was set to be 200 V/cm, with a duty ratio of 50 % at 25 Hz. In the plot, the shrinkage behaviors with DC 140, 200 V/cm, square wave of 140 V/cm at 25 Hz, and by conventional sintering without an electric field are also shown for comparison. The limiting current was set to be 150 mA in all fields. Figure 2(a) shows a flash event occurred at 1000 °C with the AC pulse as expected, which is very similar to the furnace temperature with a DC 140 V/cm field. In contrast, a flash event occurred at a lower furnace temperature with a DC 200 V/cm field. These results showed that the electric power estimation to adjust the flash temperature between the AC pulse and DC fields can be considered to be reasonable, as shown in Eq. (3).

In the case of conventional sintering, shrinkage gradually proceeds, as shown in Fig. 2(a). The shrinkage at 1000 °C was around 4 %, which is much lower than those observed with electric fields. A final shrinkage of around 16 % was obtained by the application of electric fields except for DC 200 V/cm. The final shrinkages obtained with the AC pulse, DC 140 V/cm and square pulse exhibited similar values. However, the shape difference of the waveforms affected the appearance of the sintered compacts, as shown in the optical micrographs of Figs. 2(b)–2(d). In all compacts, portions with a dark bluish color were formed on the surfaces, which meant the occurrence of reduction during flash sintering. At a glance, the area of the reduced portion was smallest with the DC field, as shown in Fig. 2(b). However, discharge damage was confirmed inside the compact flashed at DC 140 V/cm, as shown by the arrow in the cross section of Fig. 2(b). From the magnitude of reduction, the surface of the compact flashed with a square wave of 140 V/cm seemed to be very heavy, as shown in Fig. 2(c). These variations in appearances of the flashed compacts were considered to be closely related to the ionic flow induced by the electric field, as described later.

**Table 1** shows the density with an AC pulse at 200 V/cm, 50 % and 25 Hz when the limiting current was varied in the range from 100 to 300 mA. The obtained density exhibited a maximum value at 150 mA. Hereafter, the details obtained with an AC pulse at a limiting current of 150 mA will be explained.

**Figures 3**(a) and 3(b) show the duty ratio and the frequency dependency of the shrinkage behaviors during flash sintering with an AC pulse, respectively. In Fig. 3(a), the magnitude of the electric field of the AC pulse was adjusted to ensure the electric power was constant, from Eq. (3), when the duty ratios were changed. All compacts exhibited almost the same flash temperature of around 1000 °C, as expected from Eq. (3). As shown in the plot, the final shrinkages exhibited a duty ratio dependency. Final shrinkages slightly varied and showed a maximum at a duty ratio of 30 %, as indicated by the blue line in Fig. 3(a). Figure 3(b) shows the frequency dependency of the linear shrinkages when the duty ratio and electric field

Table 1. Limiting current dependency of density at 200 V/cm, 50 % and 25 Hz

| Limiting current (mA) | 100 | 150 | 200 | 300 |
|---|---|---|---|---|
| Density (g/cm$^3$) | 4.88 | 5.42 | 5.3 | (4.82)* |

*Discharges occurred.

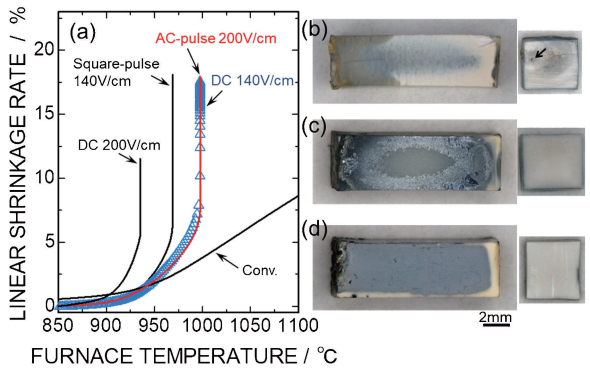


Fig. 2. Shrinkage behaviors during flash sintering with the respective electric fields as a function of furnace temperature (a) and optical micrographs of appearance and cross section of DC 140 V/cm (b), square-pulse of 140 V/cm (c), and AC pulse of 200 V/cm (d).

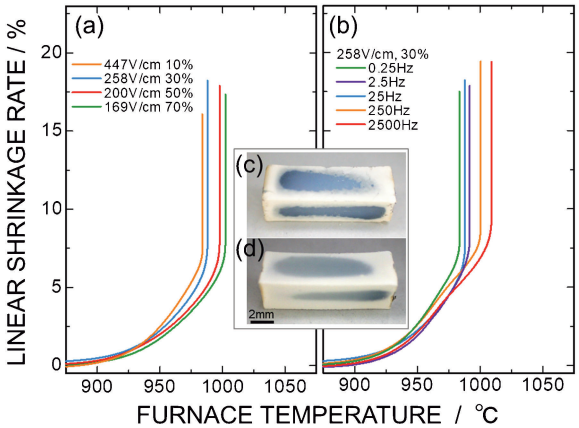


Fig. 3. Shrinkage behaviors against furnace temperature, (a) duty ratio dependence and (b) frequency dependence. Inset optical micrographs showing (c) 25 Hz and (d) 2500 Hz.

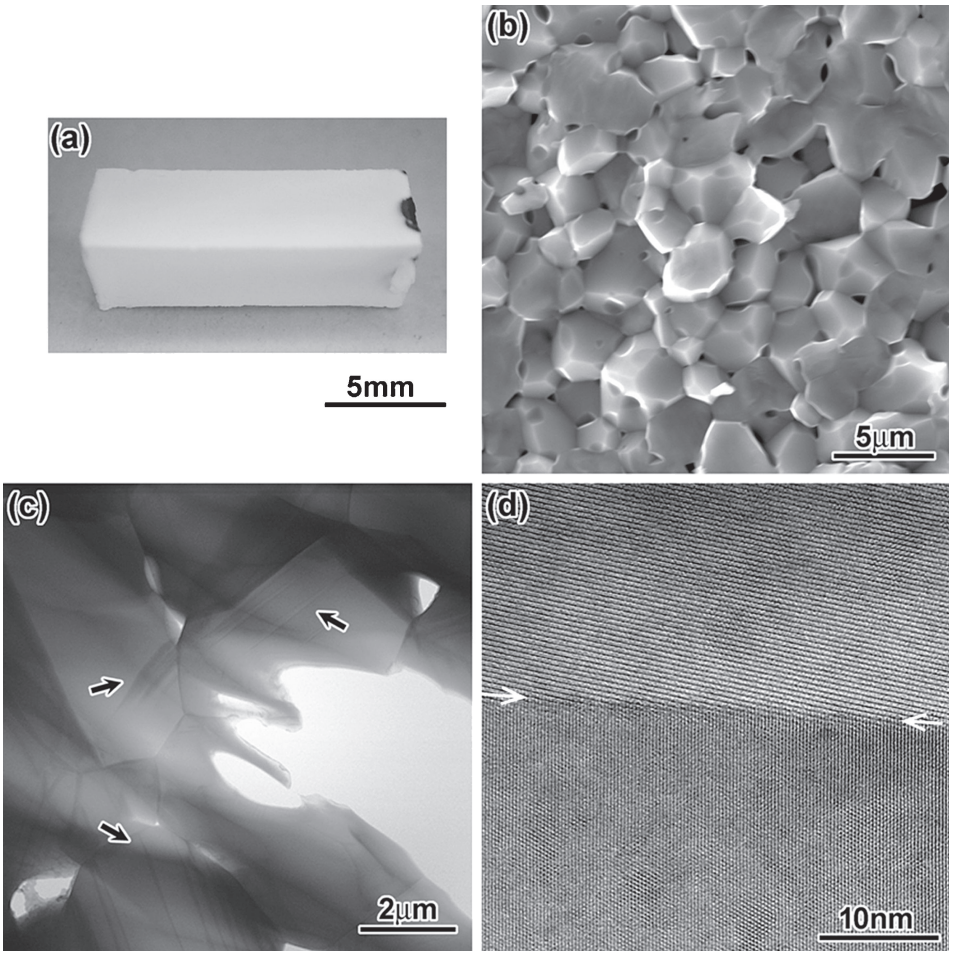


Fig. 4. Microstructure analysis results performed for $BaTiO_3$ flash sintered at furnace temperature of 1000 °C with an AC pulse of 258 V/cm, duty ratio of 30 %, and 250 Hz, (a) appearance of flash sintered $BaTiO_3$, (b) SEM image taken from fractured surface, (c) TEM bright field image showing domain contrast as indicated by arrows, and (d) HRTEM image in the vicinity of a grain boundary as indicated by the arrows.

were set at 30 % and 258 V/cm, respectively. As can be seen, the flash temperatures did not change largely around 1000 °C when the frequencies were varied. The final shrinkage at 250 and 2500 Hz were almost the same and that at 25 Hz was slightly smaller. The optical micrographs of Figs. 3(c) and 3(d) show the appearances of the respective compacts flashed at 25 and 2500 Hz. The appearance at 250 Hz is shown in **Fig. 4**(a). In both the compacts obtained at 25 and 2500 Hz, severe damages owing to reduction do not occur. The area of the portion with a white color increased; however, a pale bluish color was still seen in both compacts.

Figure 4 presents the microstructure analysis performed for the compact flashed at an AC pulse of 250 Hz and 30 % [an orange line of Fig. 3(b)]. As shown in Fig. 4(a), a flashed compact with a fully white color was obtained. This color was very similar to that obtained from the conventionally sintered compact. The actual density of this compact measured by the Archimedes method was 5.75 $g/cm^3$, which was a relative density of 95.5 % using a theoretical density of 6.02 $g/cm^3$. It should be noted that this density was obtained as a bulk value only after removing the Pt sheets used for electrodes by hands. The average grain size was estimated to be approximately 2.6 μm, as shown in Fig. 4(b). A domain structure showing a tetragonal phase was observed in the TEM bright field image shown in Fig. 4(c) and the grain boundaries were free from any amorphous or secondary phases, which was confirmed in the high resolution TEM image shown in Fig. 4(d).

**Figure 5** shows XRD profiles obtained from (a) a flashed compact shown in Fig. 4(a), and (b) a flashed compact with DC field using conditions sufficient to induce discharge. As shown in the profile of Fig. 5(b), the peaks assigned as a hexagonal phase were confirmed in the case of a DC field, which meant the actual temperature during the flash event was higher than that of the transformation temperature from cubic to hexagonal phases.[10] In contrast, the compact flashed with the AC pulse exhibited no such peaks after flashing. The estimated lattice constant was $a = 0.399$ nm and $c = 0.404$ nm, which were similar constants as conventionally sintered $BaTiO_3$.[14]

**Figure 6** shows the energy-loss near edge structure (ELNES) of Ti $L_{23}$ and O K-edges taken from the compact

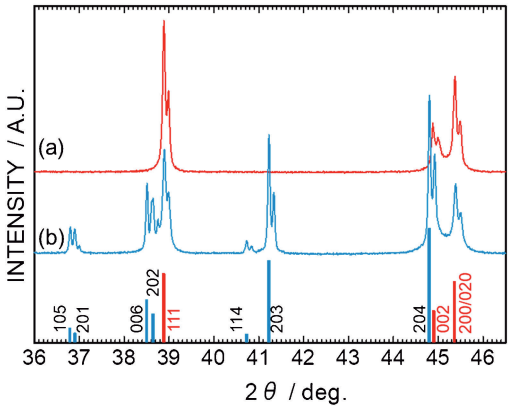


Fig. 5. XRD profiles of $BaTiO_3$ flash sintered with (a) AC pulse similar to that as shown in Fig. 4 and (b) DC electric field. Peak positions of a tetragonal phase and a hexagonal phase are indicated with red and blue lines, respectively.

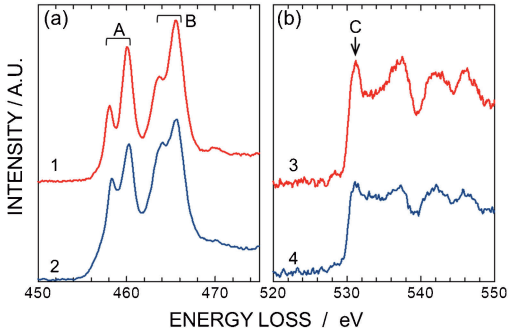


Fig. 6. (a) Ti $L_{23}$-edges and (b) O K-edges ELNES; 1 and 3 from $BaTiO_3$ flash sintered with an AC pulse similar to that in Fig. 4, and 2 and 4 from $BaTiO_3$ sintered by current-controlled consolidation process.[10]

flashed shown in Fig. 4(a). In the figure, the reference ELNES was derived from the results of a $BaTiO_3$ compact after a current-controlled consolidation process reported previously,[10] which was confirmed to be reduced. Fine structures of the Ti-$L_{23}$ and O K-edges are sensitive to the reduction of Ti ions in $BaTiO_3$. When $BaTiO_3$ is reduced, the $e_g/t_{2g}$ split in the Ti $L_{23}$-edges, as indicated by A and B, became smaller and the peak height of C decreased.[15] By comparing the fine structure in detail with each other, it can be understood that the present $BaTiO_3$ polycrystal is not reduced, which is similar to that of conventionally sintered $BaTiO_3$ reported previously.[10]

As described, to suppress reduction during flash sintering is very important. The reducing effect becomes sever under application of DC electric field as previously reported. For example, $Y_2O_3$-doped $ZrO_2$ (3YSZ) is severely reduced, which leads to a color change from white to dark blue.[16)–18)] When the reduction becomes more severe, the nitration of 3YSZ occurs even in air.[13),19)] Further, an amorphous phase appears along the grain boundaries in pure $ZrO_2$, which results from the formation of oxygen vacancies along grain boundaries.[20)] The formation of excess oxygen vacancies arising from DC electric fields often retards the shrinkage behavior. This effect is closely related to the decrease in diffusion flux because the increment of oxygen vacancy content results in a decrease in the content of cation vacancies from the viewpoint of a Schottky defect reaction. For example, when an electric field in the FAST range is applied during sintering of $BaTiO_3$, the linear shrinkage is initially enhanced; however, the final shrinkage is limited. When the electric field is removed in the sintering process, shrinkage proceeds to the final density that is obtained by conventional sintering.[10] The reduction effect arises from the one-directional flow of oxygen ions induced by a DC field.[13),16)–20)] Thus, the waveform used for flash sintering can be considered to be very important from the viewpoint of the formation of a uniform microstructure.[19)] In this study, a unique waveform including a zero-field duration was used, as shown in Fig. 1. This waveform consisted of a DC component at A and a zero-field duration at B. The zero-field duration at B was related to recovering excess oxygen vacancies generated by the DC component at A, in which the respective actual duration time depended on the frequency of the AC pulse used. As shown in Figs. 3(c) and 3(d), and Fig. 4(a), the optimal condition was around 250 Hz in the AC-pulse condition used in the present study. The balance between duration time of A and B play an important role under the AC-pulse condition.

## 4. Conclusions

Shrinkage behavior during flash sintering was investigated for $BaTiO_3$ green compacts when an alternating square current field including a zero-field duration was used. The obtained results are as follows.

1) The dark bluish color, which characterizes reduction induced by electric fields, was confirmed to decrease by using an alternating square current field including a zero-field duration. The area of the dark bluish portion was found to be sensitive to the actual duration time of the DC and zero-field components.
2) A $BaTiO_3$ sintered polycrystal with a density of 5.75 g/cm$^3$ (relative density of 95.5 %) could be obtained at the furnace temperature of 1000 °C by the optimal conditions of 258 V/cm, duty ratio of 30 % and 250 Hz.
3) TEM observation revealed no discharge and no amorphous film or secondary phase at the grain boundary and EEL analysis confirmed no occurrence of reduction.

Acknowledgments A part of this work was financially supported by Adaptable and Seamless Technology Transfer Program (A-STEP: JPMJTS1617) CREST (JPMJCR1996) from Japan Science and Technology Agency (JST) and JSPS KAKENHI (Grant Number JP19H05788).

## References

1) M. Cologna, B. Rashkova and R. Raj, *J. Am. Ceram. Soc.*, 93, 3556–3559 (2010).
2) M. Biesuza and V. M. Sglavoa, *J. Eur. Ceram. Soc.*, 39,

115–143 (2019).
3) M. Yu, S. Grasso, R. Mckinnon, T. Saunders and M. J. Reece, *Adv. Appl. Ceram.*, 116, 24–60 (2017).
4) H. Yoshida, Y. Sakka, T. Yamamoto, J. M. Lebrun and R. Raj, *J. Eur. Ceram. Soc.*, 34, 991–1000 (2014).
5) M. Cologna, J. S. C. Francis and R. Raj, *J. Eur. Ceram. Soc.*, 31, 2827–2837 (2011).
6) J. C. M'Peko, J. S. C. Francis and R. Raj, *J. Eur. Ceram. Soc.*, 34, 3655–3660 (2014).
7) A. Uehashi, H. Yoshida, T. Tokunaga, K. Sasaki and T. Yamamoto, *J. Ceram. Soc. Jpn.*, 123, 465–468 (2015).
8) H. Yoshida, A. Uehashi, T. Tokunaga, K. Sasaki and T. Yamamoto, *J. Ceram. Soc. Jpn.*, 124, 388–392 (2016).
9) D. K. Lee and H. I. Yoo, *Solid State Ionics*, 144, 87–97 (2001).
10) Y. Nakagawa, H. Yoshida, A. Uehashi, T. Tokunaga, K. Sasaki and T. Yamamoto, *J. Am. Ceram. Soc.*, 100, 3843–3850 (2017).
11) D. E. Rase and R. Roy, *J. Am. Ceram. Soc.*, 38, 102–113 (1955).
12) H. Arend and L. Kihlborg, *J. Am. Ceram. Soc.*, 52, 63–65 (1969).
13) N. Morisaki, H. Yoshida, K. Matsui, T. Tokunaga, K. Sasaki and T. Yamamoto, *Appl. Phys. Lett.*, 109, 083104 (2016).
14) W. J. Merz, *Phys. Rev.*, 76, 1221–1225 (1949).
15) G. Y. Yang, G. D. Lian, E. C. Dickey, C. A. Randall, D. E. Barber, P. Pinceloup, M. A. Henderson, R. A. Hill, J. J. Beeson and D. J. Skamser, *J. Appl. Phys.*, 96, 7500–7508 (2004).
16) C. A. Grimley, A. L. G. Prette and E. C. Dickey, *Acta. Mater.*, 174, 271–278 (2019).
17) R. E. W. Casselton, *J. Appl. Electrochem.*, 4, 25–48 (1974).
18) M. Biesuz, L. Pinter, T. Saunders, M. Reece, J. Binner, V. Sglavo and S. Grasso, *Materials*, 11, 1214 (2018).
19) T. Kurachi, Y. Yamashita, T. Tokunaga, H. Yoshida and T. Yamamoto, *J. Am. Ceram. Soc.*, 103, 3002–3007 (2020).
20) N. Morisaki, H. Yoshida, T. Kobayashi, T. Tokunaga and T. Yamamoto, *J. Am. Ceram. Soc.*, 101, 3282–3287 (2018).